NASA/TM—1999-209054

New Materials for EMI Shielding

James R. Gaier
Glenn Research Center, Cleveland, Ohio

Prepared for the
International Symposium on Electromagnetic Compatibility
sponsored by the Institute of Electrical and Electronics Engineers
Seattle, Washington, August 2–6, 1999

National Aeronautics and
Space Administration

Glenn Research Center

April 1999

Available from

NASA Center for Aerospace Information
7121 Standard Drive
Hanover, MD 21076
Price Code: A03

National Technical Information Service
5285 Port Royal Road
Springfield, VA 22100
Price Code: A03

NEW MATERIALS FOR EMI SHIELDING

James R. Gaier
National Aeronautics and Space Administration
Glenn Research Center
Cleveland, Ohio 44135

ABSTRACT

Graphite fibers intercalated with bromine or similar mixed halogen compounds have substantially lower resistivity than their pristine counterparts, and thus should exhibit higher shielding effectiveness against electromagnetic interference. The mechanical and thermal properties are nearly unaffected, and the shielding of high energy x-rays and gamma rays is substantially increased. Characterization of the resistivity of the composite materials is subtle, but it is clear that the composite resistivity is substantially lowered. Shielding effectiveness calculations utilizing a simple rule of mixtures model yields results that are consistent with available data on these materials.

INTRODUCTION

Much of the electromagnetic compatibility analysis on fiber reinforced plastic composites has assumed that the fibers utilized will have been optimized for structural strength (PAN-based carbon fibers) rather than for electrical performance. These analyses have indicated that composites lack the shielding effectiveness required for many high performance applications. Substituting fibers that have been optimized for elastic modulus (pitch-based fibers) substantially increases the shielding effectiveness because the fibers are more highly crystalline and hence have higher electrical conductivity. If fibers that have been optimized for thermal conductivity (second generation pitch-based fibers and vapor grown fibers) are used the shielding effectiveness increases even more because the electrical conductivity of these fibers is even higher. But if the essential property is electrical conductivity, then the fibers used should be optimized for it.

Electrical resistivity of highly crystalline carbon fibers (pitch-based and vapor-grown) can be substantially lowered through the process of intercalation, the insertion of guest atoms or molecules between the graphene layers (refs. 1 and 2) (fig. 1). Thus, a sensible approach appears to be to incorporate these intercalated graphite fibers in shielding materials. This paper reviews the work that NASA has carried out to investigate the effects of intercalated graphite fibers on shielding effectiveness of composite materials.

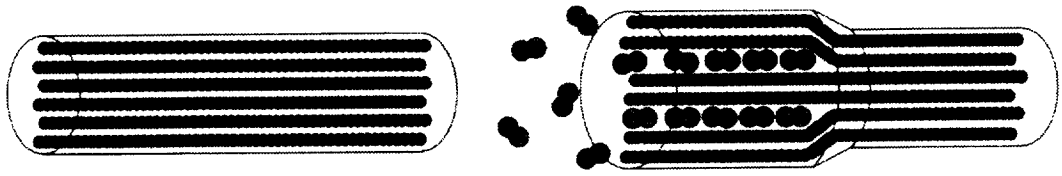

Figure 1 -- Intercalation is the insertion of guest atoms or molecules between the graphene layers.

CHOICE OF FIBER AND INTERCALATE

There are a wide variety of carbon fibers available from many manufacturers with a wide range of properties. Furthermore, manufacturers continuously refine their processes and, since the electrical resistivity is not their primary property of interest, the resistivity of a fiber type may vary depending on when the fiber was made. NASA centered its attention on fibers developed by Union Carbide (now Amoco) because it was a large domestic source with a wide product line. Numerous attempts in our lab and others have led to the conclusion that Amoco's PAN-based fibers are not crystalline enough to be intercalated. However, both pitch-based and vapor grown fibers can be intercalated by a wide variety of intercalates. Carbon fibers which are crystalline enough to form intercalation compounds will be referred to here as graphite fibers.

The primary characteristic that led to the intercalate choice was stability. Most of the early work in graphite intercalation compounds was done using crystalline graphite and alkali metals such as lithium, potassium, and cesium. These compounds decompose within seconds on contact with air or water (ref. 3). Transition metal chlorides such as $FeCl_3$, $CuCl_2$, and $NiCl_2$ proved to form intercalation compounds with graphite fibers which were stable in air, but would also decompose in water vapor. The class of intercalates which proved to form the most stable compounds, at least in graphite fibers, were the halogens, Br_2, ICl, and IBr.

Although the resistivity of these three intercalation compounds is similar, most of the work done at NASA has centered around fibers with Br_2 as the intercalate because it intercalates most graphite fibers at room temperature, and appears to have the most stable intercalation compounds (ref. 4). The resulting fiber is about 18 percent Br_2 by mass with an average empirical formula of about $C_{50}Br$. The Br_2 is concentrated towards the middle of the fiber, with none detectable (<5 percent by EELS, SAM analysis) on the fiber surface. The Br_2 intercalation process is less damaging than that of most other intercalates, so the degradation in mechanical (ref. 5) and thermal properties (ref. 6) is minimal.

Most of the studies were carried out using P-100 fibers (Amoco's designation for its pitch-based fibers with a 100 msi elastic modulus) because it was the most crystalline production fiber available when these studies started. A substantial number of studies were also carried out with P-55 and P-75 fibers to study the effects of crystalline order on the properties. Studies have also been carried out with vapor-grown fibers from a number of sources (General Motors, General Atomic, Showa Denko, and Applied Sciences), but until recently the reproducibility of the fibers has been poor and they have not been available in even prototyping quantities. The resistivity of graphite fibers and their Br_2 graphite intercalation compounds are shown in table I.

Table I -- Resistivity of Graphite Fibers

Fiber Type	Pristine μΩ-cm	Br_2 GIC μΩ-cm
PAN (T-300)	2000	N/A
P-55	900	300
P-75	500	100
P-100	250	50
Vapor Grown	75	7

INTERCALATED GRAPHITE FIBER/POLYMER COMPOSITES

Graphite fibers are not used alone but as part of a composite. Although a wide variety of matrices are available, NASA's interest has centered around polymer matrices. Most of the composites studied have utilized either epoxy or polycyanate ester matrices. These polymeric resins are highly resistive, and since most laminar composites have a practical maximum fiber volume of about 60 percent, there is a concomitant loss in

conductivity. The use of conductive resins results in little lowering of the composite resistivity because the matrix is still at least four orders of magnitude more resistive than the fibers (ref. 7).

The determination of the resistivity of a composite material is a subtle art, dependent upon the technique used. For example, when the ASTM standard test for measuring surface and volume resistivities is used, values up to ten orders of magnitude higher than those predicted from a simple rule of mixtures model, or as measured by four-point or eddy current techniques are obtained (ref. 8).

Four-point techniques often yield results with poor reproducibility if great care is not taken making the electrical contacts. Removing the surface resin layer by sanding or similar techniques results in the breakage of fibers, which then interrupts their contact with the fiber network or may even cause them to fall out of the composite. Current contacts are important to ensure a uniform injection of the current into the composite. Painting over all surfaces near the end of the composite with silver paint, wrapping a thin copper wire several times around the painted area, and then applying a second coat of silver paint has been effective. Voltage contacts of silver paint dots or lines painted parallel to the equipotential surface have both been effective. The reproducibility of the measurement can be improved significantly by using a multipoint contact. In this variation of the four-point method, several voltage contacts are painted on the surface and measured in all possible pair-wise combinations. If the voltage between pairs is plotted as a function of distance between the points times the current divided by the cross-sectional area, the slope of the resulting line is the resistivity. A least squares fit to the data give consistent values for the resistivity.

Eddy current resistivities are measured using commercially available equipment. Care must be taken that the skin depth is much greater than the sample thickness for the measurement to be meaningful. The skin depth is a function of both the conductivity of the sample and the frequency of the radiation, with lower frequency having a larger skin depth. At NASA the samples are measured using a 55.55 kHz instrument and samples are typically 1 mm thick. This technique enables resistivities between about 10^2 and 10^5 $\mu\Omega$-cm to be measured.

It is not apparent exactly how the eddy current resistivity should be interpreted. Eddy current theory assumes a homogeneous medium, and the composites are heterogeneous on a variety of scales. Macroscopically, the fibers have a resistivity of about 50 $\mu\Omega$-cm and they are embedded in a matrix that has a resistivity of about 10^{13} Ω-cm. The fiber diameter is about 10 μm, and they are separated by distances which vary along the length of fibers from contact to spacings up to 1 μm. The microstructure of the fiber itself is not homogeneous containing crystallites with a characteristic length of about 200 Å embedded in somewhat amorphous regions. If the fiber is intercalated with Br_2, the distribution of Br_2 is not uniform. In general, there is no detectable bromine on the surface, and up to stage two (two carbon layers per Br_2 layer) in the interior. Some sections of the fiber contain more Br_2 than others (ref. 9). Finally, the conversion of conductivity to resistivity to compare the results of the two techniques assumes that the off-diagonal elements of the conductivity tensor are zero, which may or may not be the case.

The complexities of resistance analysis can be illustrated by comparing two suites of experiments. In the first, (ref. 10) current was fed into one corner of a 28×28 cm, one mm thick, four-ply composite of 0° to 90° woven fabric. Current was bled out through a second contact located at positions that made an angle with the fabric that varied from 0° to 90° in 15° increments. The voltage gradient across the composite was mapped by 36 voltage probes in a square pattern across the surface. An example of the resulting gradient pattern for the P-100+Br_2 composite is shown in figure 2. The pattern was the same as that made by similar measurements made on a brass plate of the same dimensions. It was thus concluded that, on a cm scale at least, composites made from 0° to 90° woven fabrics act electrically like isotropic plates.

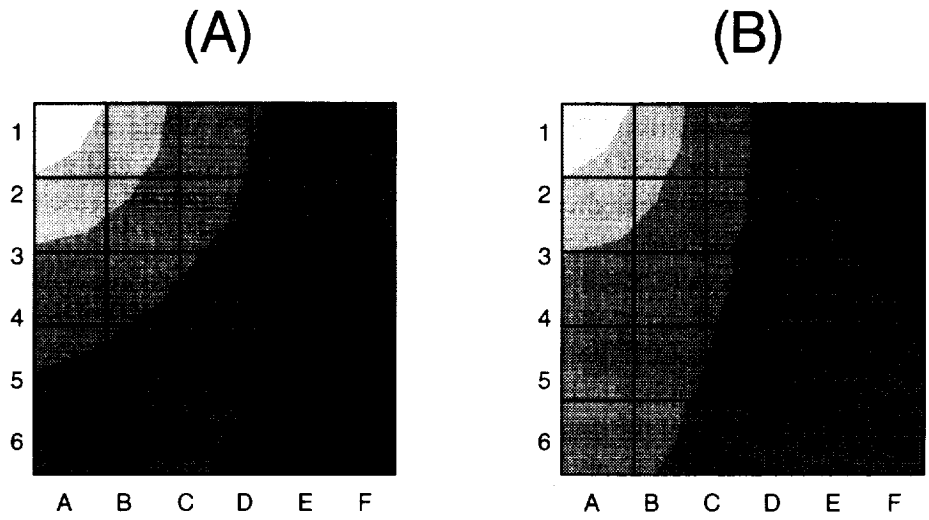

Figure 2 -- Electrical potential contours in 5 mV increments on a P-100+Br_2/polycyanate ester composite where the current is injected at the top left corner and bled out of (A) the bottom right corner, 45° to the weave, and (B) the top right corner, parallel to the weave.

However, when multipoint measurements were made on strips of the same type of composite that were only 1.0 cm wide and about 10 cm long, the results were very anisotropic (ref. 11). Those composites which had a current direction at an angle to the weave direction, had a considerably higher resistivity. They in fact showed an angular dependence (fig. 3) indicating that they acted as though the current would run down a fiber length, and then cross over to a perpendicular fiber, effectively increasing the composite's length by a factor of (|sin θ| + |cos θ|).

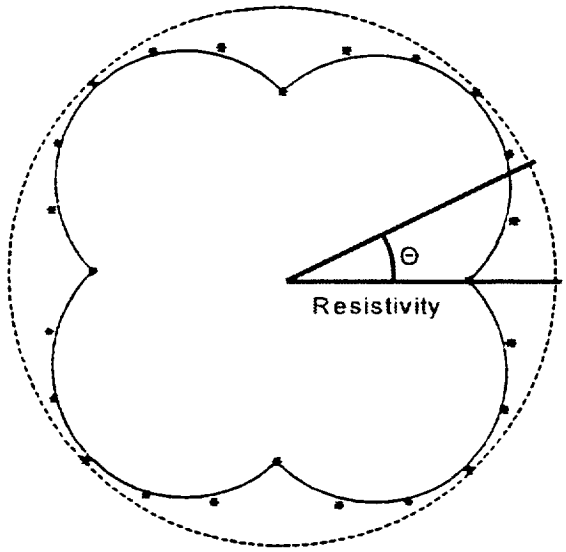

Figure 3 -- Polar plot of the angular dependence of the resistivity for composite strips cut at various angles to the 0°-90° weave direction as predicted by the (|sin θ| + |cos θ|). Multipoint data is indicated by "✱", and eddy current resistivity is indicated by the dashed circle.

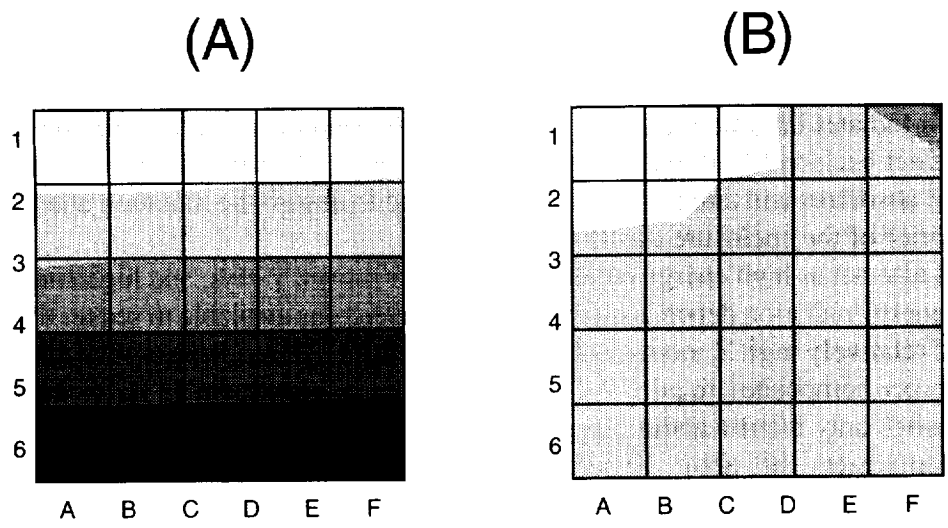

Figure 4 -- Electrical potential contours in 5 mV increments on a PAN/P-100+Br_2/polycyanate ester resin composite laid up 0°-0°-0°-0° where the current is injected at the top left corner and bled out of (A) the bottom right corner, 45° to the weave, and (B) the top right corner, parallel to the weave.

The resistivity of composites that are designed to be anisotropic have additional complexities. A composite which was made with high resistivity PAN fibers in the warp direction and low resistivity P-100+Br_2 fibers in the weave direction show a preferred direction of current flow (fig. 4). This was as expected. However, a peculiar local effect observed that appears to be "negative resistivity" (the white area in fig. 4(b)) was certainly not expected and remains, at this time, unexplained.

EMI shields must perform other functions besides fending off EMI, so how does the process of intercalation effect other properties? As mentioned earlier, Br_2 does not greatly disturb the microstructure of the fibers. Thus the mechanical and thermal properties of composites made from these materials do not differ from composites made from pristine fibers. Table II compares the properties of P-100/epoxy and P-100+Br_2/epoxy to aluminum. Extrapolations from this table lead to the conclusion that if shielding effectiveness can be maintained, equal thickness shielding could result in a 62 percent mass savings, equal strength shielding a 72 percent mass savings, and equal stiffness shielding in a 94 percent mass savings. Clearly, there is the promise of significant mass savings here.

TABLE II -- Composite Properties

Property	6061 Al	P-100/epoxy	P-100+Br_2/epoxy
Electrical Resistivity	3.5 μΩ-cm	570 μΩ-cm	140 μΩ-cm
Tensile Strength	0.52 Gpa	1.6 x Al	1.6 x Al
Young's Modulus	71 Gpa	6 x Al	6 x Al
CTE	23 ppm/K	-1.6 ppm/K	-1.6 ppm/K
Thermal Conductivity	24.7 W/m-K	10 x Al (in plane)	10 x Al (in plane)
Thermal Emittance (1000 nm)	0.02	0.91	0.91
Density	2.71 g/cm^3	0.61 x Al	0.66 x Al

How do the thermal characteristics of these composites compare with Al? When a component generates heat in a spacecraft it radiates infrared radiation to the shield. Aluminum is a good reflector in the infrared and the heat tends to reflect back and forth within the box raising the temperature near the component. Graphite composites are good absorbers and emitters of infrared and tend to absorb the radiation and re-radiate it which would keep the interior of the enclosure cooler (ref. 12).

EMI shields also act as high energy radiation shields for x-rays, γ-rays, and high energy particles. The ability to stop high energy radiation depends on the number of electrons available to scatter them. Intercalation, with its addition of relatively high Z atoms, enhances the ability to shield from x-rays and γ-rays (ref. 13). Pristine graphite/epoxy composites require 2.4 times the mass of aluminum to have equal shielding. Br_2 intercalated composites only require about 60 percent of the mass of Al to provide equal shielding, and IBr intercalated fiber composites only about 30 percent of the mass. Thus, if the EMI shields are limited by the radiation environment, intercalation is required to improve on aluminum.

EMI SHIELDING EFFECTIVENESS OF COMPOSITES

For the purposes of this discussion EMI is defined as any electromagnetic radiation, periodic or random, that has a disturbing influence on devices exposed to it. Only radiation which is propagated through space will be considered. Disturbances which travel along power or ground paths will not be considered since shielding from such disturbances involves the installation of filtering devices rather that passive materials.

The shielding effectiveness calculations used were adapted from a NASA Special Publication by Taylor (ref. 14) though there are many other sources available. An inherent assumption about the equations used is that the conductivity of the shielding material is isotropic, which as indicated above is not true for these materials. These calculations do form a zero order approximation from which to begin. Further details of the calculations are available elsewhere (ref. 15).

Shielding effectiveness of 1.0 mm thick plates of two metals, aluminum and copper, and seven graphite fiber polymer composites with 50 percent fiber fill, three of which utilize intercalated graphite fibers, were made. Composite resistivity is assumed to be twice that of the fibers. The resistivity values used in the calculations are shown in table III (ref. 15).

The total attenuation of EMI (in dB) is the sum of three terms, absorption, reflection, and internal reflection. The frequency dependence of the three terms is illustrated in figure 5 for the far field (where the source to shield distance is large with respect to the wavelength of the radiation) for a 1.0 mm Cu plate. There is a frequency above which the absorption dominates and the shielding effectiveness increases rapidly with frequency. For Cu that occurs near 1 MHz. The frequency of the rapid increase is important, for above that properties other than shielding effectiveness should dominate design considerations.

Figure 6 shows a plot of the far field shielding effectiveness of a 1.00 mm thick plate of each of the nine materials as a function of frequency. The minimal frequency at which the shielding effectiveness of the material reaches 200 dB (SE_{200}) reveals some instructive trends. First, Cu and

TABLE III -- Resistivity Values Used in EMI Shielding Calculations

Material	Resistivity, μΩ-cm
Copper	1.8
Aluminum	2.8
P-100+Br_2 composite	100
P-75+Br_2 composite	200
P-55+Br_2 composite	600
P-100 composite	500
P-75 composite	1000
P-55 composite	1800
PAN composite	4000

Al are far superior to the composites in shielding effectiveness, with the SE_{200} occurring 3.5 orders of magnitude lower than conventional PAN composites, and nearly two orders of magnitude lower than the most conductive intercalated graphite composites. Second, intercalation lowers the SE_{200} by about an order of magnitude. Third, P-100+Br_2 has an SE_{200} nearly two orders of magnitude below that of PAN composites making it suitable for shielding in the GHz regions where PAN composites are not. This makes a compelling case to reconsider many shielding applications for which it has been thought composites were not suitable.

Figure 7 is a similar plot to figure 6, but for the near field case, dominated by the electric field vector. This occurs when the noise source operates at high voltage and low current. This calculation assumes that the noise source is located 10 cm from the shield, and so the specifics of the frequency distribution cannot be extrapolated too far, but it is yet instructional. The overall shape of the frequency distribution differs from the far field case in that the shielding effectiveness is high both at low frequencies and at high frequencies, with a trough in between that is dependent both on the material and the source distance. The low point for both Al and Cu are higher than 100 dB, and so are not shown in this figure. Decreasing the resistivity has two effects on the trough. It becomes shallower and it shifts to lower frequency. If shielding effectiveness values below 100 dB are unacceptable, then PAN fiber composites could not be used in this regime at frequencies higher than 20 MHZ. P-100+Br_2 fiber composites could be used for all frequencies except within a 0.10 to 25 GHz window. If 75 dB was required, then PAN fiber composites could not be used above 100 MHZ, but P-100+Br_2 fiber composites could be used over all frequency ranges.

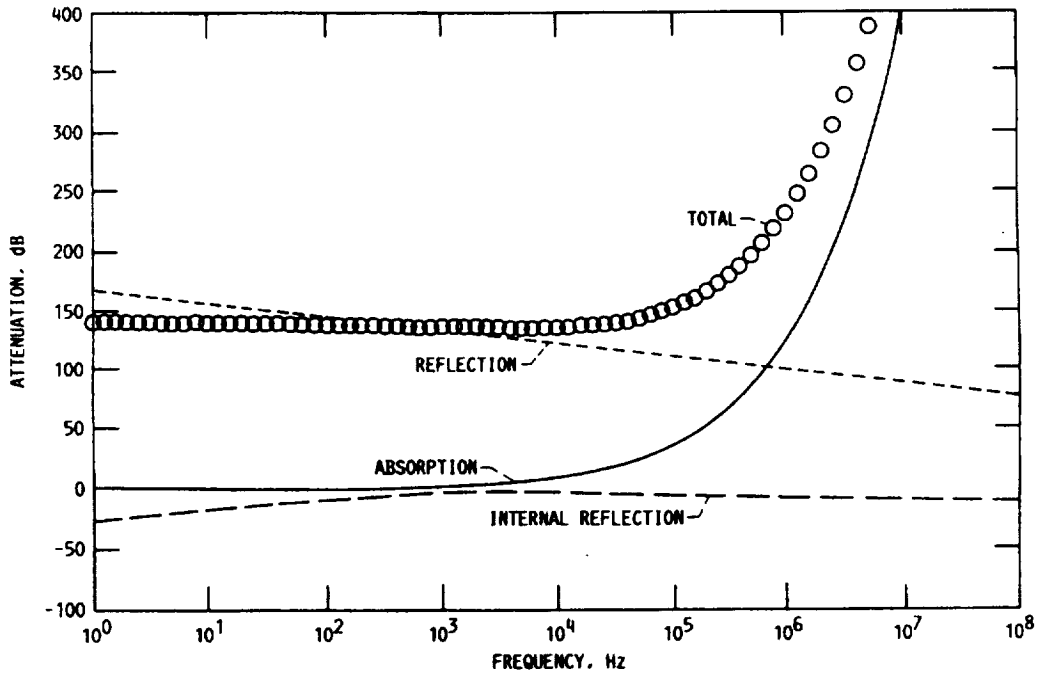

Figure 5 -- Contributions from absorption, reflection, and internal reflection to the total far field shielding effectiveness of 1 mm thick copper as a function of frequency.

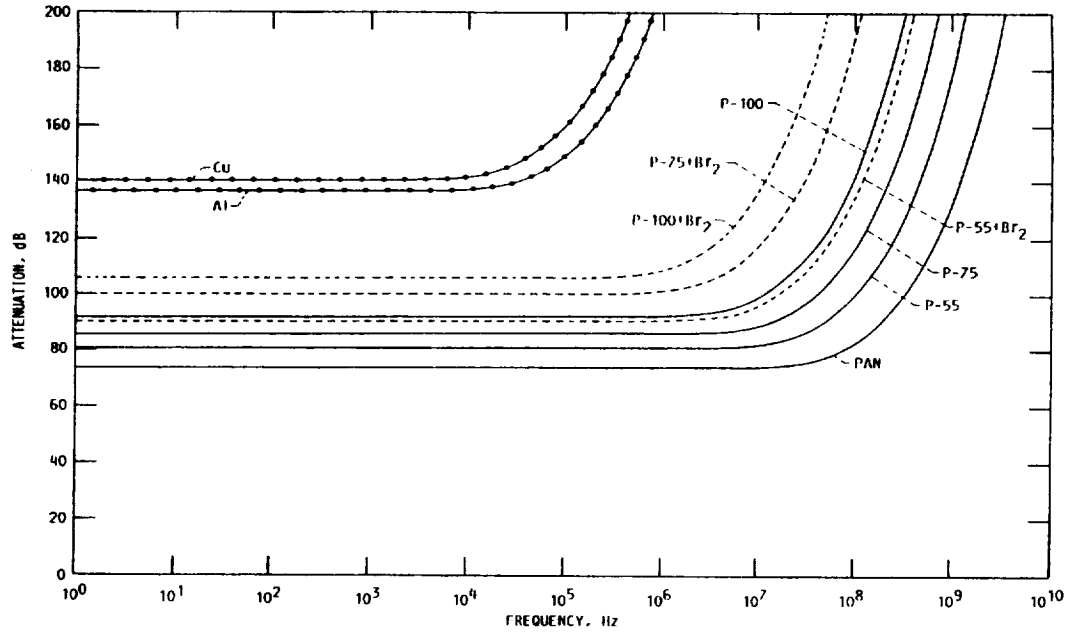

Figure 6 -- Calculated shielding effectiveness of metals (connected circles), graphite fiber composites (solid lines) and Br_2 intercalated graphite fiber composites (dashed lines) in the far field.

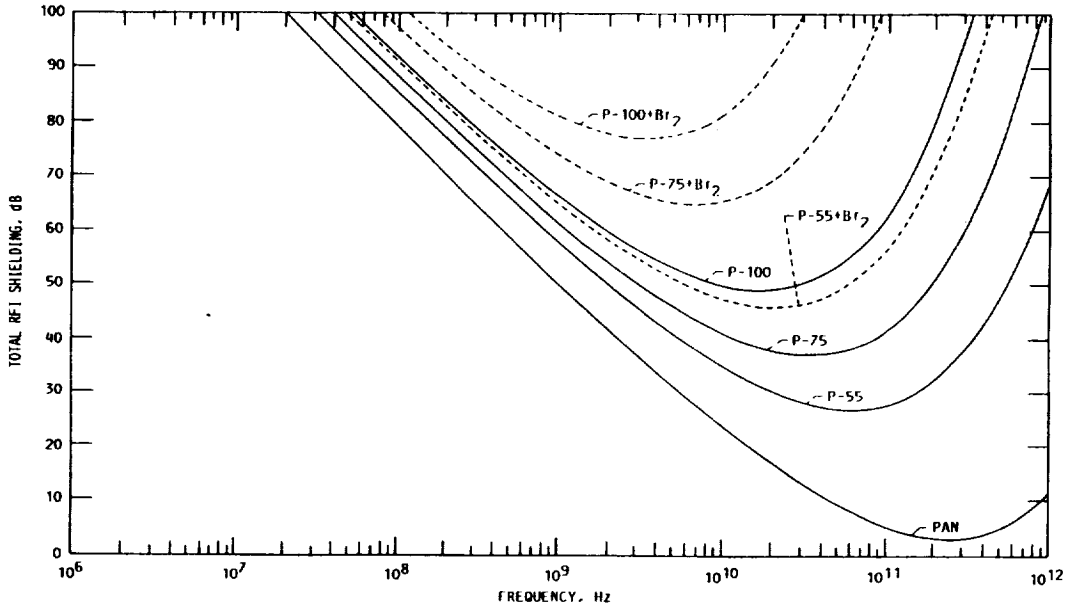

Figure 7 -- Calculated shielding effectiveness of graphite fiber composites (solid lines) and Br_2 intercalated graphite fiber composites (dashed lines) in the electric field dominated near field when the source distance is 10 cm.

Figure 8 is a plot similar to the last two but in the near field when it is dominated by the magnetic field vector, which occurs when the noise source operates at high current and low voltage. This is the type of shielding that is required near power sources. Once again, this is for a noise source that is located 10 cm from the shield, and so the particulars of the frequency distribution change with distance. Note that none of the materials is suitable for this application. Only materials with high magnetic permeability have sufficient shielding.

These calculations were admittedly flawed from the outset by the assumption of the materials being homogeneous. Do the calculations bear any resemblance to experimental evidence? A series of coupon tests have been run at several different facilities in several frequency ranges. All of them have one limitation in common, and that is that it is very difficult to measure high levels of shielding effectiveness. Four-ply samples of P-55, P-75, P-100, P-75+Br_2 and P-100+Br_2 were evaluated at Ferro Corporate Research Facilities (Independence, OH). Both far field and near field measurements were made between 30 and 1000 MHz. The experimental limit on the apparatus was 55 dB, and all samples shielded to at least that level in the far field. The calculations indicate that P-55 at 1000 MHz should have the lowest shielding effectiveness and that it should be about 57 dB. The near field measurements indicated that the shielding effectiveness was somewhat less than predicted, but experimental artifacts call the data into question. In addition, the far field attenuation of a 0.75 mm P-100+Br_2 composites was evaluated in the McDonnell-Douglas (St. Louis) mixed mode chamber in the frequency range of 1 to 12 GHz. The shielding effectiveness exceeded 70 dB, the range of this instrument. Thus, although there is no firm experiment data giving exact values, the results are so far consistent with the calculations.

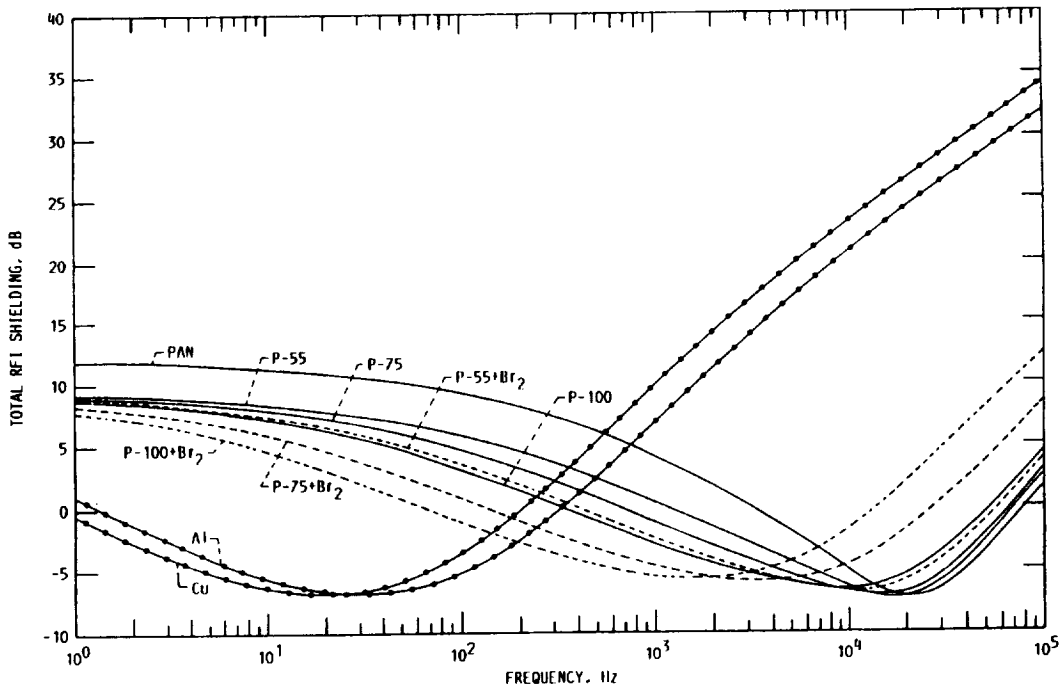

Figure 8 -- Calculated shielding effectiveness of metals (connected circles), graphite fiber composites (solid lines), and Br_2 intercalated graphite fiber composites (dashed lines) in the magnetic field dominated near field when the source distance is 10 cm.

In actual applications more complex shapes will be required than simple flat coupons. In an attempt to determine the shielding effectiveness of an actual enclosure, a five sided box with dimensions 37×8×8 cm with a 2 cm mating surface was fabricated at Hughes Space and Communications (Los Angles) from six plies of P-100+Br_2, and bolted to their test fixture using a standard EMI shielding gasket, where it was tested in the far field over a frequency range of 0.1 to 1000 MHz. The results, shown in figure 8, indicate that the attenuation exceeded 70 dB over the entire range.

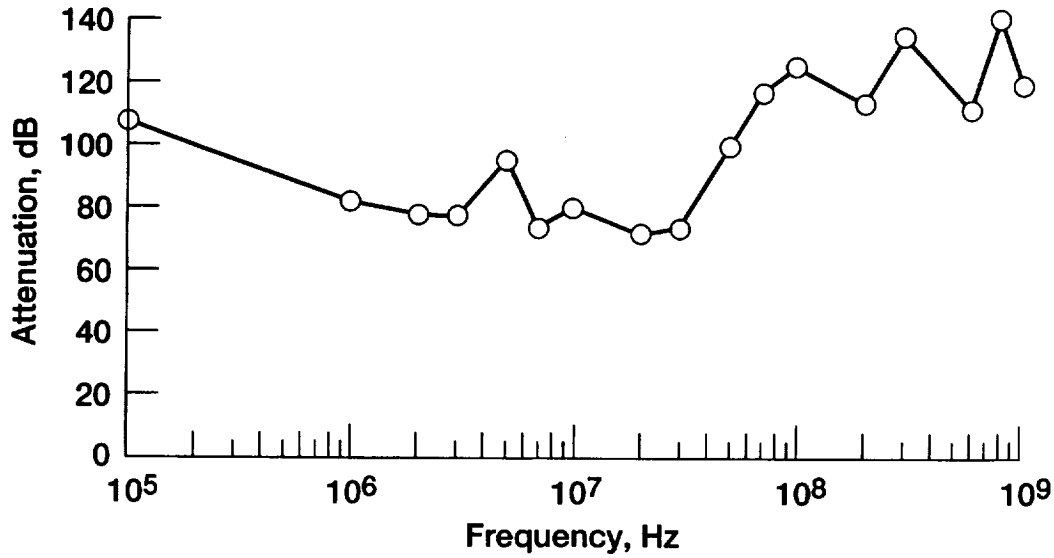

Figure 9 -- Measured shielding effectiveness of a five-side P-100+Br_2/polycyanate ester composite box (courtesy of Hughes Space and Communications Co., Los Angeles).

CONCLUSIONS

A new class of graphite fibers which have been optimized for electrical conductivity is a technology that could enable the use of composite EMI shields, enabling a significant decrease in their mass. Bromine intercalation is an effective way to decrease the resistivity of fibers, and so their composites, while retaining the mechanical and thermal properties of the graphite fibers. In addition, intercalation with IBr can significantly enhance the ability of graphite polymer composites to shield electrons from high energy x-ray and γ-rays. Characterizing the resistivity of the composites is subtle, and the spreading of current throughout the composites is not well understood, but rough calculations of the resistivity using the rule of mixtures yield shielding effectiveness values which are consistent with experimental measurements to date.

REPORT DOCUMENTATION PAGE

Form Approved
OMB No. 0704-0188

1. AGENCY USE ONLY (*Leave blank*)	2. REPORT DATE	3. REPORT TYPE AND DATES COVERED
	April 1999	Technical Memorandum

4. TITLE AND SUBTITLE

New Materials for EMI Shielding

5. FUNDING NUMBERS

WU-632-1A-1E-00

6. AUTHOR(S)

James R. Gaier

7. PERFORMING ORGANIZATION NAME(S) AND ADDRESS(ES)

National Aeronautics and Space Administration
John H. Glenn Research Center at Lewis Field
Cleveland, Ohio 44135-3191

8. PERFORMING ORGANIZATION REPORT NUMBER

E-11590

9. SPONSORING/MONITORING AGENCY NAME(S) AND ADDRESS(ES)

National Aeronautics and Space Administration
Washington, DC 20546-0001

10. SPONSORING/MONITORING AGENCY REPORT NUMBER

NASA TM—1999-209054

11. SUPPLEMENTARY NOTES

Prepared for the International Symposium on Electromagnetic Compatibility sponsored by the Institute of Electrical and Electronics Engineers, Seattle, Washington, August 2–6, 1999. Responsible person, James R. Gaier, organization code 5480, (216) 433–6686.

12a. DISTRIBUTION/AVAILABILITY STATEMENT

Unclassified - Unlimited
Subject Categories: 24 and 33 Distribution: Nonstandard

This publication is available from the NASA Center for AeroSpace Information, (301) 621–0390.

12b. DISTRIBUTION CODE

13. ABSTRACT ***(Maximum 200 words)***

Graphite fibers intercalated with bromine or similar mixed halogen compounds have substantially lower resistivity than their pristine counterparts, and thus should exhibit higher shielding effectiveness against electromagnetic interference. The mechanical and thermal properties are nearly unaffected, and the shielding of high energy x-rays and gamma rays is substantially increased. Characterization of the resistivity of the composite materials is subtle, but it is clear that the composite resistivity is substantially lowered. Shielding effectiveness calculations utilizing a simple rule of mixtures model yields results that are consistent with available data on these materials.

14. SUBJECT TERMS

Electromagnetic; Intercalation; Composites; Resistivity

15. NUMBER OF PAGES

17

16. PRICE CODE

A03

17. SECURITY CLASSIFICATION OF REPORT	18. SECURITY CLASSIFICATION OF THIS PAGE	19. SECURITY CLASSIFICATION OF ABSTRACT	20. LIMITATION OF ABSTRACT
Unclassified	Unclassified	Unclassified	

REFERENCES

1. H. Oshoma, J.A. Woolam, and A. Yavrouian, *J. Appl. Phys.* ***53(12)***, 9220 (1982).

2. T.C. Chieu, M.S. Dresselhaus, and M. Endo, *Phys. Rev B* ***26***, 5867 (1982).

3. F.A. Cotton and G. Wilkinson Advanced Inorganic Chemistry, 5th Ed. (John Wiley & Sons, Inc., New York, 1988) 238.

4. J.R. Gaier, M.E. Slabe and N. Shaffer, *Carbon* ***26***, 381 (1988).

5. D.A. Jaworske, R.D. Vanucci, and R. Zinolabedini, *J. Composite Materials* ***21***, 580 (1987)

6. C-C. Hung and J. Miller, NASA Technical Memorandum 88863 (1986).

7. J. Gaier, NASA Technical Memorandum 103632 (1990)

8. *Unpublished results* J.R. Gaier, NASA Lewis Research Center (1987), J. Lenhoff, Triton Systems (1997).

9. X.W. Qian, S.A. Soiln, and J.R. Gaier, *Phys. Rev. B* ***35***, 2436 (1987).

10. J.R. Gaier, S.P. Berkebile, *Manuscript in progress*, abstracted in 24th Biennial Conference on Carbon (1999)

11. J.R. Gaier and Y. Yoder, 4th International Conference on Composite Engineering, (International Composites Community, New Orleans, 1997) 343.

12. J.R. Gaier and J. Terry, Seventh International Materials and Processing Conference (Society for the Advancement of Materials and Processing, Covina, CA, 1994) 221.

13 J.R. Gaier, W.C. Hardebeck, J.R. Terry Bunch, M.L. Davidson, and D.B. Berry, *J. Mater. Res* ***13***, 2297, (1998).

14. R.E. Taylor Radio Frequency Interference Handbook NASA SP-3067 (1971).

15. J.R. Gaier, *IEEE Transactions on Electromagnetic Compatibility*, 351 (1992).